

## A Mechanism of the Onset of the South Asian Summer Monsoon

Daisuke MINOURA, Ryuichi KAWAMURA

*Department of Earth Sciences, Toyama University, Toyama, Japan*

and

Tomonori MATSUURA

*National Research Institute for Earth Science and Disaster Prevention, Tsukuba, Japan*

*(Manuscript received 30 August 2002, in revised form 25 February 2003)*

### Abstract

Using the European Centre for Medium-Range Weather Forecasts reanalysis data, we examine whether an onset mechanism of the Australian summer monsoon proposed by Kawamura et al., which incorporates possible air-sea feedback processes, can apply to the South Asian summer monsoon system as well. In their mechanism, a combination of the increase in sea surface temperatures and dry intrusion into the layer at 600–850 hPa level over the ocean off, the equatorial side of a continent, plays a crucial role in enhancing potentially convective instability prior to the onset. It is found that the onset mechanism is able to apply to the abrupt onset of the Indian summer monsoon at the beginning of June, rather than the earliest onset over the Indochina peninsula in middle May. This is consistent with the observational fact that abruptness of the monsoon onset is most evident over the coastal regions of the Indian subcontinent. The Indochina peninsula is characterized by a relatively slow onset, although its date is earliest. The asymmetry of the transition speed between the onset and retreat regimes also has similar regional features. If the mechanism operates efficiently on the Indian subcontinent and adjacent oceans, it is anticipated that the onset of the Indian summer monsoon is delayed, as compared to that over Southeast Asia because subsidence in the periphery of a sub-continental scale thermal low, resulting from intensification of land-ocean thermal contrast, inhibits convection. This may be one of the possible reasons why the two major onsets seen in the South Asian summer monsoon system are clearly distinguished from each other.

### 1. Introduction

Why does monsoon onset occur abruptly (where onset is defined as the beginning of organized deep cumulus convection, i.e., monsoonal rainfall)? It has long been known that the regime transition of monsoon circulation suddenly occurs from pre-onset to post-onset,

and conversely, it tends to be less abrupt at the time of monsoon retreat. A number of researchers have described the Asian monsoon and its sudden seasonal changes (e.g., Krishnamurti and Ramanathan 1982; Lau and Li 1984; Murakami and Nakazawa 1985; He et al. 1987; Lau et al. 1988; Yanai et al. 1992; Li and Yanai 1996; Hsu et al. 1999). Several possible mechanisms have already been presented to account for the abruptness of the onset: (1) dry/moist (conditional) symmetric instability of zonal monsoon flows (Krishnakumar and Lau 1998), (2) a switch from one dynamical regime to the other due to seasonally varying sea surface

---

Corresponding author: Ryuichi Kawamura, Department of Earth Sciences, Toyama University, 3190 Gofuku, Toyama 930-8555, Japan.  
E-mail: kawamura@sci.toyama-u.ac.jp  
© 2003, Meteorological Society of Japan

temperature (SST) forcing (Yano and McBride 1998), (3) the delay of the formation of a thermally direct circulation, due to geostrophic balance, and associated moist baroclinic instability (Xie and Saiki 1999), and (4) a sort of sub-critical instability from the equatorial trough flow regime to the monsoon trough flow regime (Chao 2000).

The presence of a continent influences low-level circulations over its surrounding ocean through increased land-ocean thermal contrast, resulting in anomalous SST and surface ocean currents prior to the monsoon onset. Wind-induced SST anomalies may in turn influence the behavior of deep cumulus convection at the onset phase. Such a continent forcing effect has not been addressed in the onset mechanisms stated above. More recently, Kawamura et al. (2002) examined the abrupt transition of the Australian summer monsoon circulation from pre-onset to post-onset regimes, using an atmospheric reanalysis data aided by an ocean general circulation model, and proposed an onset mechanism that incorporates possible air-sea feedback processes. This mechanism is briefly described as follows.

A well-organized, continental-scale shallow vertical circulation over the Australian continent results from rapid intensification of land-ocean thermal contrast during the premonsoon period. The shallow vertical circulation is dynamically coupled both with a thermally-induced low at the lower level below 850 hPa, and a thermal high at 600–700 hPa level. Westerly wind stress anomalies appear due to geostrophic balance over the Arafura Sea and Timor Sea north of the Australian continent, implying the weakening of easterlies. SST over those regions increases as a result of reduced surface evaporation, and increased solar radiation in a less-cloudy air induced by the subsidence in the periphery of the thermal low. On the other hand, the thermal high brings about increased dry advection from extratropical regions, particularly from the dry Australian continent. The well-organized nature of the shallow vertical circulation associated with the thermal high, leads to dry intrusion into the layer at about 700 hPa over the Arafura Sea and Coral Sea, through the horizontal and vertical advective processes. A combination of the SST increase and the dry intrusion creates

a more potentially unstable condition. While subsidence suppresses convection, potentially convective instability is further enhanced prior to monsoon onset owing to the above effect. The arrival of large-scale disturbances with ascending motion (such as the Madden-Julian oscillation) at the domain where the lower troposphere is potentially unstable triggers deep cumulus convection, indicating the onset of the monsoon.

Their onset mechanism is valid for Australia, located in the subtropics, that is a comparatively small and round-shaped continent without complicated topography. However, one may wonder whether it can apply to other monsoon systems that have continental masses in the subtropics. For instance, the Asian continent, which has high mountains and complicated topography, is much larger than the Australian continent and is not very isolated from other continents. He et al. (1987) showed that the Asian summer monsoon is characterized by two successive monsoon onsets: i.e., middle May over Southeast Asia, and early June over India. Such complicated features cannot be seen in the Australian summer monsoon system (e.g., Nicholls et al. 1982; Lubis and Murakami 1984; Holland 1986; Suppiah 1992). It is uncertain whether Kawamura et al.'s onset mechanism can apply to the two abrupt transitions of the South Asian summer monsoon system. One may also wonder whether the two transitions occur due to different mechanisms.

This study focuses specifically on the two successive onsets of the South Asian summer monsoon system. The main objectives of this study are to: (1) validate whether the onset mechanism proposed by Kawamura et al. (2002) can apply to the South Asian summer monsoon, and (2) examine why the South Asian summer monsoon undergoes the two successive onsets in middle May and early June. Section 2 describes the data used and analysis procedure. Section 3 describes the regional differences of the time evolution of the South Asian summer monsoon. Section 4 examines the horizontal and vertical structures of the monsoon circulation at pre-onset and post-onset regimes. The spatial patterns of SST and convective instability are presented in Section 5. Finally, discussion and summary are given in Sections 6 and 7, respectively.

## 2. Data and analysis procedure

Datasets used in this study include: (1) the European Centre for Medium-Range Weather Forecasts (ECMWF) reanalysis (ERA) data with a spatial resolution of  $2.5^\circ \times 2.5^\circ$ , (2) weekly outgoing longwave radiation (OLR) data with a spatial resolution of  $2.5^\circ \times 2.5^\circ$  observed from NOAA satellites (which provides an appropriate measure of deep cumulus convection in the tropics), and (3) weekly sea surface temperature (SST) data with a spatial resolution of  $1^\circ \times 1^\circ$  compiled by Reynolds and Smith (1994). We used all the data for the period 1982–1993 and the ERA data for analysis as weekly mean values to compare it to the other observational data. These weekly data are useful in examining the detailed features of the two successive monsoon onsets. Since the analyzed period is not necessarily long enough to obtain climatological mean values, sampling fluctuations owing to a shortage of data are not disregarded. Thus, a low-pass time filter is applied to the weekly mean data without exception.

The monsoon system, which is highly seasonal, is characterized by a zonally asymmetric circulation (due to large land-ocean thermal contrast), whereas the midlatitude circulation has a strong zonally symmetric component and less seasonality. For instance, looking at the Australian continent, its southern portion is dominated by the midlatitude circulation system. Since the midlatitude system is too pronounced, the monsoon circulation over the entire continent is partly masked by the strong zonally symmetric component. To aid in the analysis of the transition of the monsoon circulation from the pre-onset regime to the post-onset regime, atmospheric and oceanic quantities are thus partitioned into zonally symmetric and asymmetric components. Zonally asymmetric anomalies  $A^*$  are defined as:

$$A^* = A' - [A'],$$

where  $A'$  represents the deviation from the annual mean of an atmospheric or oceanic quantity  $A$ ;  $[A']$  is the zonal average of  $A'$ .  $A^*$  is expected to be useful for understanding the monsoon circulation with a distinctive zonally asymmetric component and strong seasonality. The weekly mean quantities used are based on

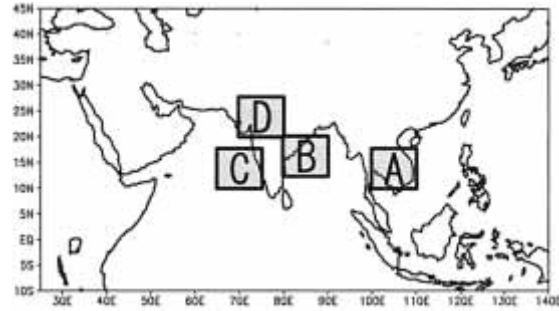


Fig. 1. Four regions selected for examining the seasonal evolutions of OLR: Region A ( $100^\circ$ – $110^\circ$ E,  $10^\circ$ – $17.5^\circ$ N), Region B ( $80^\circ$ – $90^\circ$ E,  $12.5^\circ$ – $20^\circ$ N), Region C ( $65^\circ$ – $75^\circ$ E,  $10^\circ$ – $17.5^\circ$ N), and Region D ( $70^\circ$ – $80^\circ$ E,  $20^\circ$ – $27.5^\circ$ N).

the climatology of 1982–1993. The above procedure is the same as that applied to Kawamura et al. (2002).

## 3. Regional differences of monsoon onset

To first understand the regional differences of the South Asian summer monsoon onset, four regions are selected shown in Fig. 1. Region A ( $100^\circ$ – $110^\circ$ E,  $10^\circ$ – $17.5^\circ$ N) is selected as a representative region of Southeast Asia, Region B ( $80^\circ$ – $90^\circ$ E,  $12.5^\circ$ – $20^\circ$ N) is the western portion of the Bay of Bengal, including part of the eastern coast of the Indian subcontinent, Region C ( $65^\circ$ – $75^\circ$ E,  $10^\circ$ – $17.5^\circ$ N) is the eastern portion of the Arabian Sea, including part of the western coast of the subcontinent, and Region D ( $70^\circ$ – $80^\circ$ E,  $20^\circ$ – $27.5^\circ$ N) is an inland area of the subcontinent.

Figure 2 shows the seasonal evolutions of weekly mean OLR for the respective regions during the period 1982–1993, along with climatological mean OLR values. One of the common features is that abrupt onsets occur from late May to early June in Regions B and C, corresponding to the Indian summer monsoon onset, i.e., the second transition termed by He et al. (1987). The minimum values of climatological OLR are about  $190 \text{ W m}^{-2}$  and  $215 \text{ W m}^{-2}$  in Regions B and C, respectively. The abruptness of the onset can be seen almost every year, and the lines at the onset phase are parallel. Conversely, monsoon retreats occur very slowly in the two regions compared with

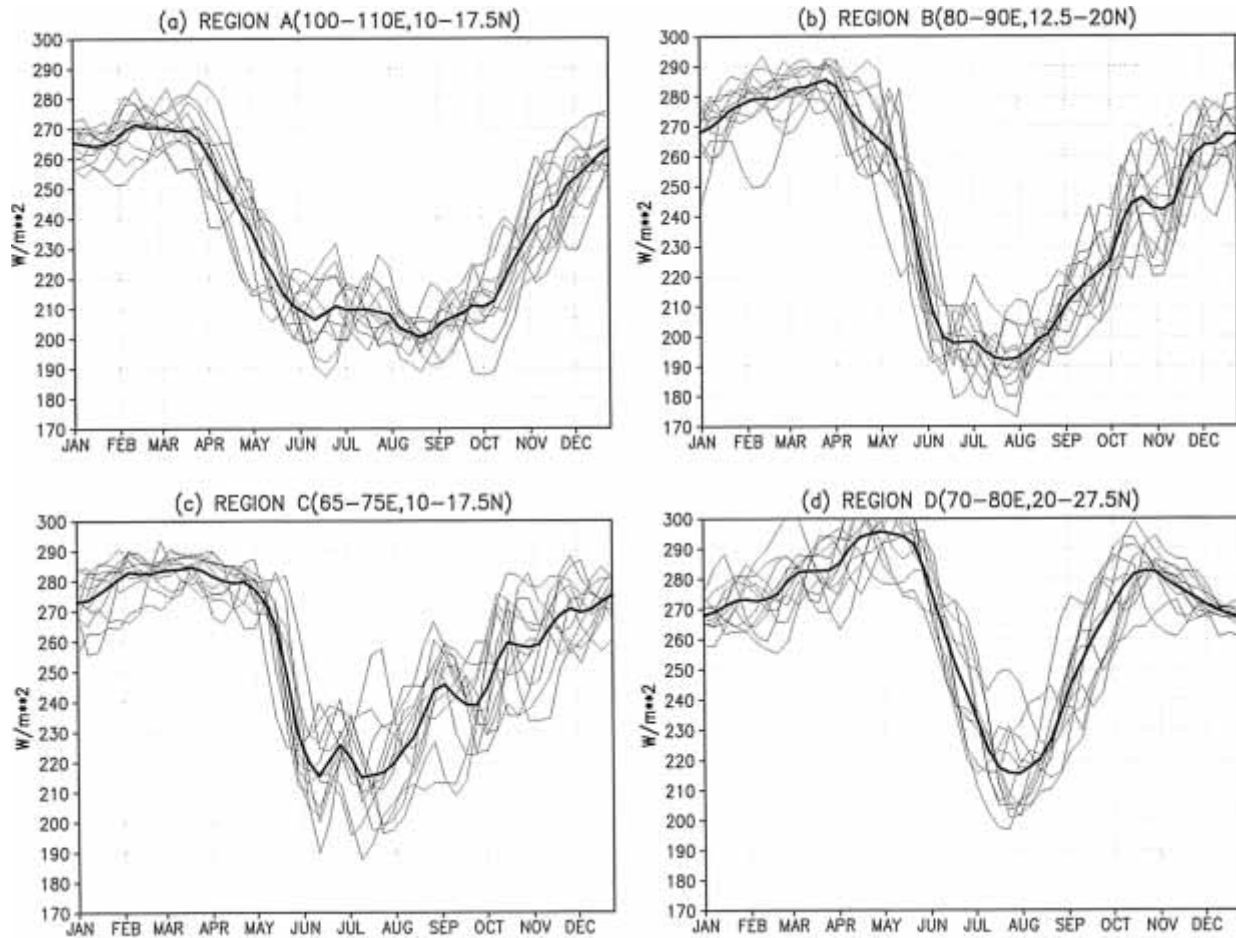


Fig. 2. Seasonal evolutions of weekly OLR for the four regions during the period 1982–1993. Climatological mean values are denoted by thick lines.

the onsets. On the other hand, Region A undergoes a comparatively slow onset, and does not have a distinctive asymmetric feature of transition speed between the onset and retreat regimes, although its onset, which is termed the first transition (He et al. 1987), occurs approximately 2–3 weeks earlier than that of the Indian summer monsoon (e.g., Matsumoto 1997). As is well known, monsoon onset in Region D occurs latest in the four regions, which reflects the seasonal northward migration of the intertropical convergence zone (ITCZ). In this region the speed of retreat is not very different from that of onset as well as Region A.

We stress here that there are considerable regional differences of both the monsoon onset and retreat in the South Asian summer mon-

soon system, which has not necessarily been addressed in the previous studies. The asymmetry of the transition speed between the onset and retreat regimes is evident in Regions B and C, but is less clear in Regions A and D. It is worthwhile to note that such an asymmetry is more prominent in the coastal areas of the Indian subcontinent (including part of adjacent ocean) than in the inland areas, which will be discussed later.

#### 4. Monsoon circulations at pre-onset and post-onset regimes

To clarify the horizontal and vertical structures of monsoon circulations at the time of the two successive onsets, the respective maps for the 16<sup>th</sup> week (April 16–22), the 18<sup>th</sup> week

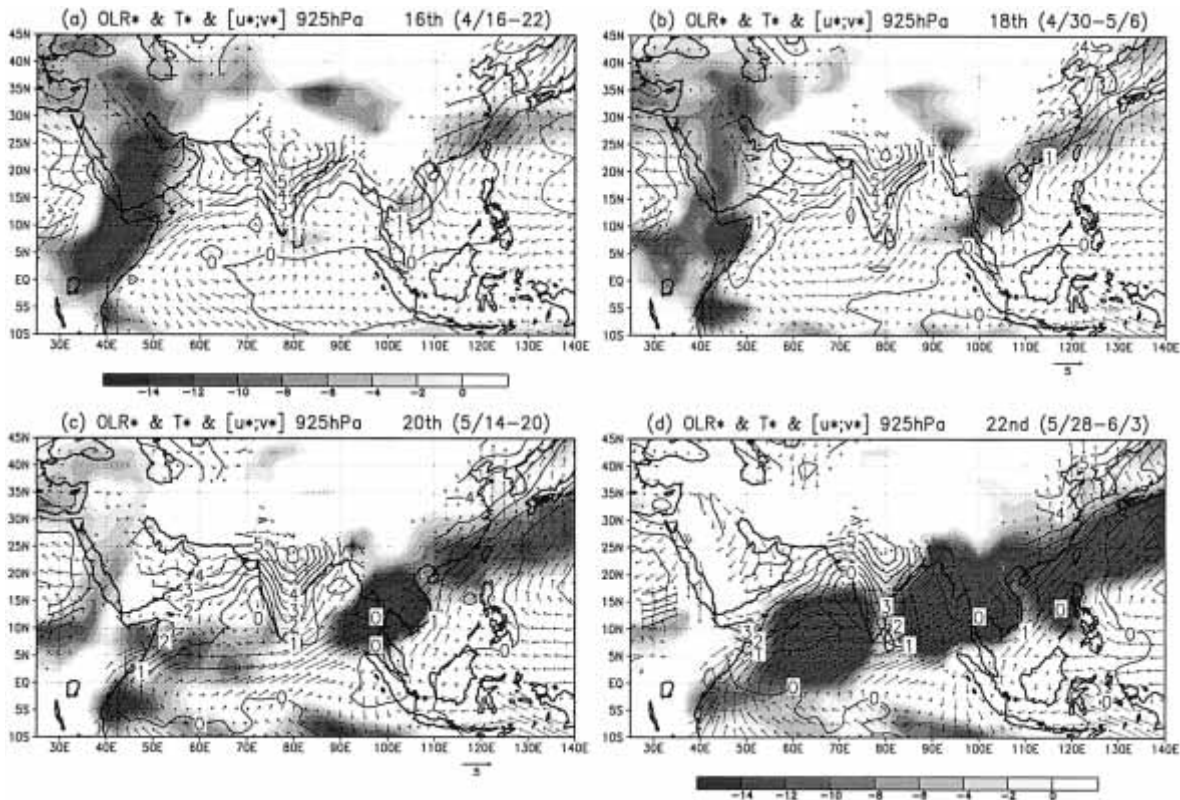


Fig. 3. Spatial patterns of anomalous 925-hPa air temperature  $T^*$ , wind vector ( $u^*, v^*$ ), and  $OLR^*$  for: (a) 16<sup>th</sup> week (April 16–22); (b) 18<sup>th</sup> week (April 30–May 6); (c) 20<sup>th</sup> week (May 14–20); and (d) 22<sup>nd</sup> week (May 28–June 3). Contour interval for temperature is  $1^\circ\text{C}$ , and reference arrow is  $5 \text{ m s}^{-1}$ . Shading denotes regions of negative  $OLR^*$  anomalies.

(April 30–May 6), the 20<sup>th</sup> week (May 14–20), and the 22<sup>nd</sup> week (May 28–June 3) are presented.

#### 4.1 Horizontal structures

Figure 3 shows the spatial patterns of anomalous 925-hPa air temperature  $T^*$ , wind vector ( $u^*, v^*$ ), and  $OLR^*$  for: (a) 16<sup>th</sup> week, (b) 18<sup>th</sup> week, (c) 20<sup>th</sup> week, and (d) 22<sup>nd</sup> week. In middle April, the Indian subcontinent is already covered by positive  $T^*$  with a value of greater than  $5^\circ\text{C}$  due to land-surface warming. Associated with this, northerly and southerly anomalies appear along the western and eastern coasts of the continent, respectively, which is dynamically linked with the dominance of geostrophic wind above the atmospheric boundary layer (surface–850 hPa). Southerly anomalies are also observed from the South China Sea to the East China Sea. Convection

over Southeast Asia (Region A) is rapidly enhanced from the beginning of May to middle May, corresponding to the first onset, and extremely active convection occurs over the Bay of Bengal and the Arabian Sea, from late May to early June, corresponding to the second onset (i.e., the onset of the Indian summer monsoon). The second onset is accompanied by pronounced southwesterly anomalies. After the onset,  $T^*$  decreases especially over the coastal regions of India.

Figure 4 shows the spatial pattern of anomalous mixing ratio  $q^*$  and moisture flux ( $qu^*, qv^*$ ) at the same level as Fig. 3. Looking at middle April, marked positive  $q^*$  exceeding  $+2 \text{ g kg}^{-1}$  is observed over the southern edge of the Indian subcontinent and over the Indochina peninsula, accompanied by northward moisture flux anomalies, indicating northward moisture supply within the boundary layer into inland.

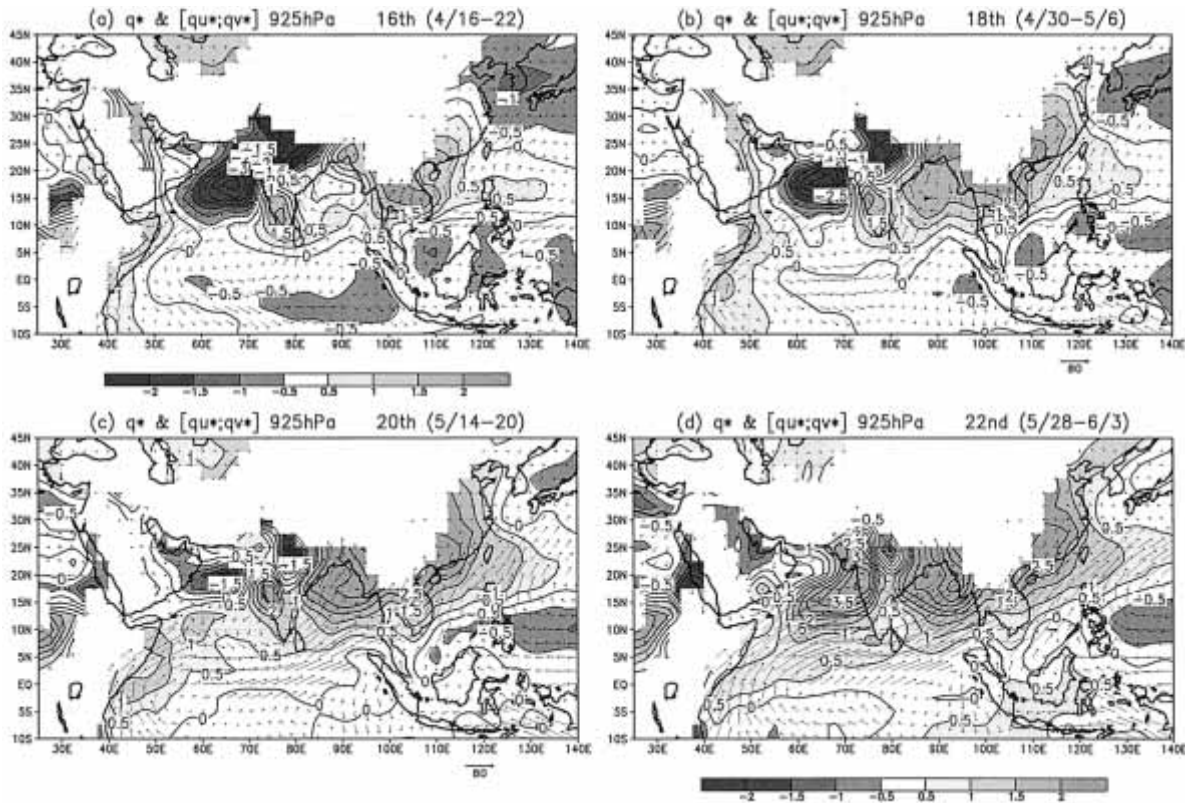


Fig. 4. As in Fig. 3 but for 925-hPa water vapor mixing ratio  $q^*$  and moisture flux ( $qu^*$ ,  $qv^*$ ). Contour interval for mixing ratio is  $0.5 \text{ g kg}^{-1}$ , and reference arrow is  $80 \text{ g kg}^{-1} \text{ m s}^{-1}$ .

The northward moisture transports over India and Southeast Asia occur along the western periphery of anticyclonic circulation anomalies over the Bay of Bengal, and the western North Pacific in the vicinity of the Philippines, respectively. These low-level anomalous anticyclonic circulations over ocean are induced, in conjunction with cyclonic circulation anomalies over land, due to enhanced land-ocean thermal contrast. In contrast, significant negative  $q^*$  accompanied by northeasterly anomalies, is indicated over the Arabian Sea and the northern portion of the subcontinent.

The two positive  $q^*$  areas seen in middle April come together in early May. It is interesting to note that the Bay of Bengal is already dominated by intense moisture in middle May, prior to the second onset. After the second onset, remarkable positive  $q^*$  also covers the eastern part of the Arabian Sea. Although the complicated topography of the Asian continent,

such as the Indian subcontinent and the Indochina peninsula, produces complicated features of increased moisture transport from tropical oceans into the continent from middle April to early June, a fundamental feature in Fig. 4, is the influx of moisture from tropical oceans starts on the southeastern periphery of the continent and expands westward into the southwestern counterpart. If a continent is located in the subtropics of the Northern Hemisphere, prior to summer monsoon onset, low-level southerly (northerly) anomalies are induced along the eastern (western) periphery of the continent, due to a large land-ocean thermal contrast (e.g., Kawamura and Murakami 1998). An anomalous oceanic anticyclone east of the continent, together with a continental-scale thermal low, plays an important role in the penetration of moist air in the lower troposphere into the inland in the eastern portion of the continent. This dynamic

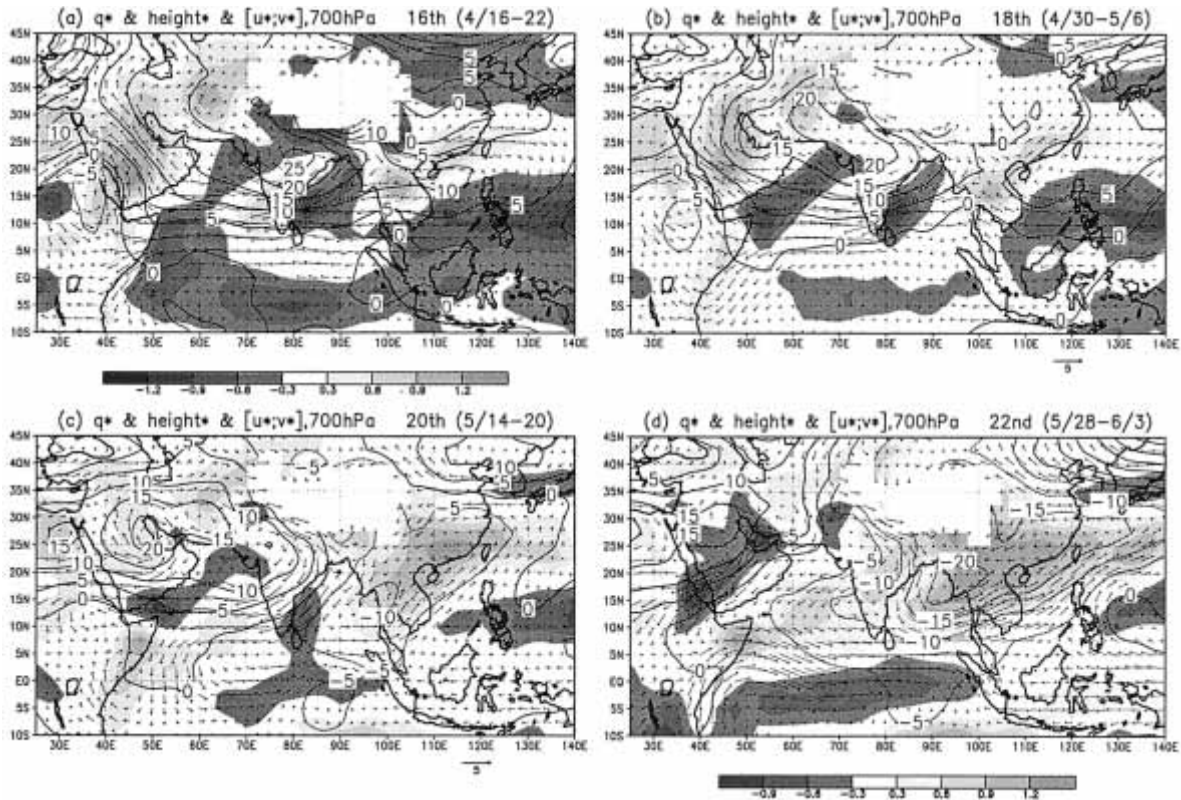


Fig. 5. As in Fig. 3 but for 700-hPa height  $z^*$ , wind vector  $(u^*, v^*)$ , and mixing ratio  $q^*$ . Contour interval for height is 5 m, and reference arrow is  $5 \text{ m s}^{-1}$ . Heavy and light shadings denote significant negative and positive mixing ratio anomalies.

process is supposed to facilitate the earliest monsoon onset over the Indochina peninsula.

The zonally asymmetric horizontal circulation at 700-hPa level is shown in Fig. 5. A remarkable anticyclonic circulation anomaly with positive  $z^*$  is found over the Indian subcontinent in middle April, which can be identified with a thermally induced high. Associated with the sub-continental scale thermal high, significant negative mixing ratio anomalies ( $q^*$ ) cover the Bay of Bengal and the Arabian Sea. On the contrary, positive  $q^*$  appears in the vicinity of Southeast Asia, and amplifies until early June, implying that the rainy season of Southeast Asia commenced. It is characteristic that the thermal high migrates westward from early May and its center reaches the African continent in early June. Nearly concurrent with the westward displacement of the thermal high, distinctive positive  $q^*$  areas become zonally elongated with a northeastward tilt, corre-

sponding well to negative  $OLR^*$  areas shown in Fig. 3. In early June, a noticeable cyclonic circulation anomaly, with increased moisture, is seen over Southeast Asian and the southern portion of China.

Although the zonally elongated positive  $q^*$  areas are indicative of well-organized deep cumulus convection is easily understood, it is unclear why both the Bay of Bengal and the Arabian Sea are characterized by negative  $q^*$  prior to the second monsoon onset. In the next subsection, the vertical structures of the monsoon circulations at pre-onset and post-onset regimes are examined to understand three-dimensional monsoon flows.

#### 4.2 Height-latitude sections

Figure 6 shows the height-latitude sections of vertical  $p$ -velocity, meridional wind and mixing ratio averaged from  $80^\circ$  to  $85^\circ\text{E}$  along the eastern coast of the Indian subcontinent for: (a)

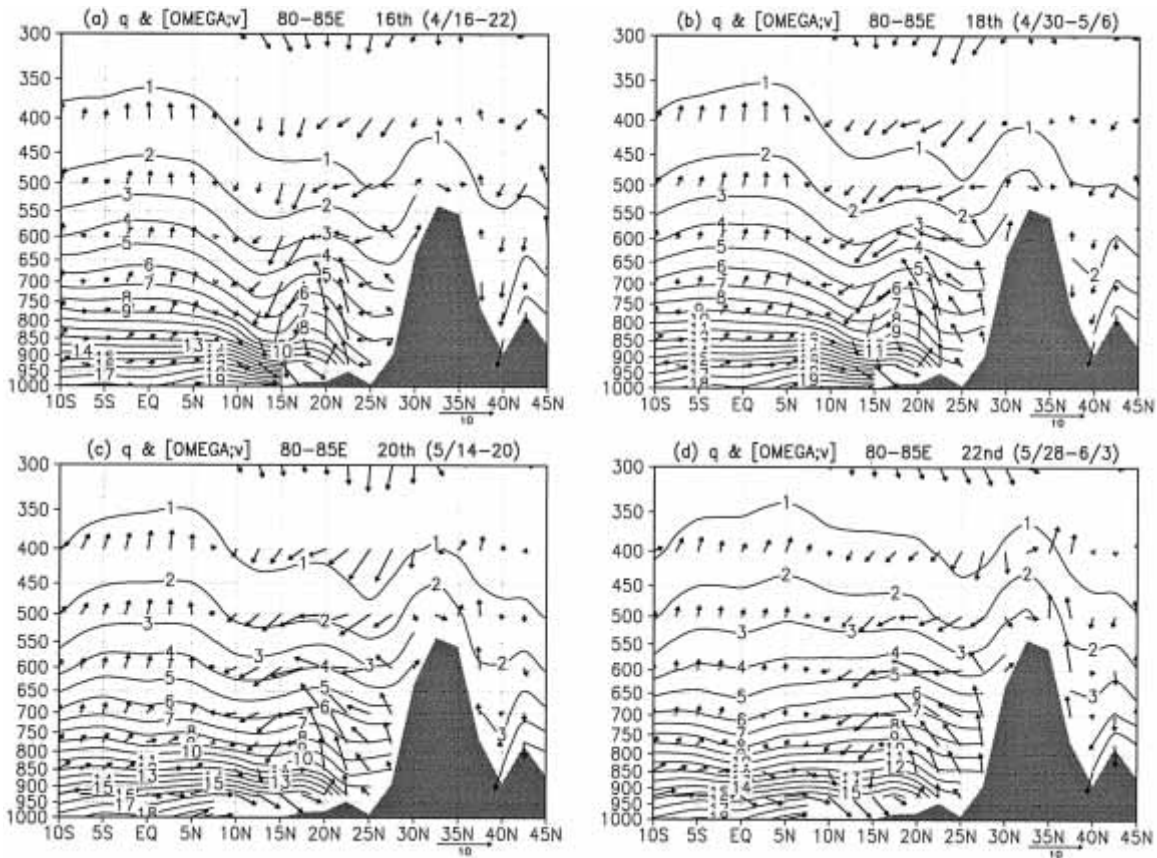


Fig. 6. Height-latitude sections of climatological mean vertical  $p$ -velocity ( $\omega$ ) and meridional wind component below 300-hPa averaged from  $80^{\circ}$  to  $85^{\circ}$ E for: (a) 16<sup>th</sup> week (April 16–22); (b) 18<sup>th</sup> week (April 30–May 6); (c) 20<sup>th</sup> week (May 14–20); and (d) 22<sup>nd</sup> week (May 28–June 3). Also shown is water vapor mixing ratio. Contour interval is  $1 \text{ g kg}^{-1}$ . The vertical motion has been exaggerated 75 times.

16<sup>th</sup> week, (b) 18<sup>th</sup> week, (c) 20<sup>th</sup> week, and (d) 22<sup>nd</sup> week. Note that the three quantities in this figure are not zonally asymmetric anomalies. A notable feature prior to the onset of the Indian summer monsoon is the presence of a shallow vertical circulation in the lower troposphere between  $10^{\circ}$  and  $25^{\circ}$ N. Ascending motion is seen over land between  $20^{\circ}$  and  $25^{\circ}$ N, whereas descending motion prevails off the eastern coast of the subcontinent between  $10^{\circ}$  and  $15^{\circ}$ N. This circulation, which is balanced by a thermal wind relation, involves a thermally induced low at the lower level below 850-hPa and a thermal high at 600–700-hPa level, and characterizes the premonsoon circulation (e.g., Xie and Saiki 1999; Kawamura et al. 2002). Subsidence over the adjacent ocean

plays an influential role in suppressing convection. As presented later, thermal forcing by land surface warming plays a crucial role in originating such a shallow vertical circulation.

The intrusion of moisture from the tropical Indian Ocean into the inland dominates in the boundary layer below about 900-hPa level, when the sub-continental scale vertical circulation develops before the Indian summer monsoon commences, whereas the descending branch between  $10^{\circ}$  and  $15^{\circ}$ N is accompanied by a relatively low mixing ratio, resulting in reinforcing the vertical gradient of mixing ratio in the lower troposphere. In all panels, upward motion is observed, especially in the upper troposphere of the tropics, implying the ascending branch of the Hadley circulation. In addition,



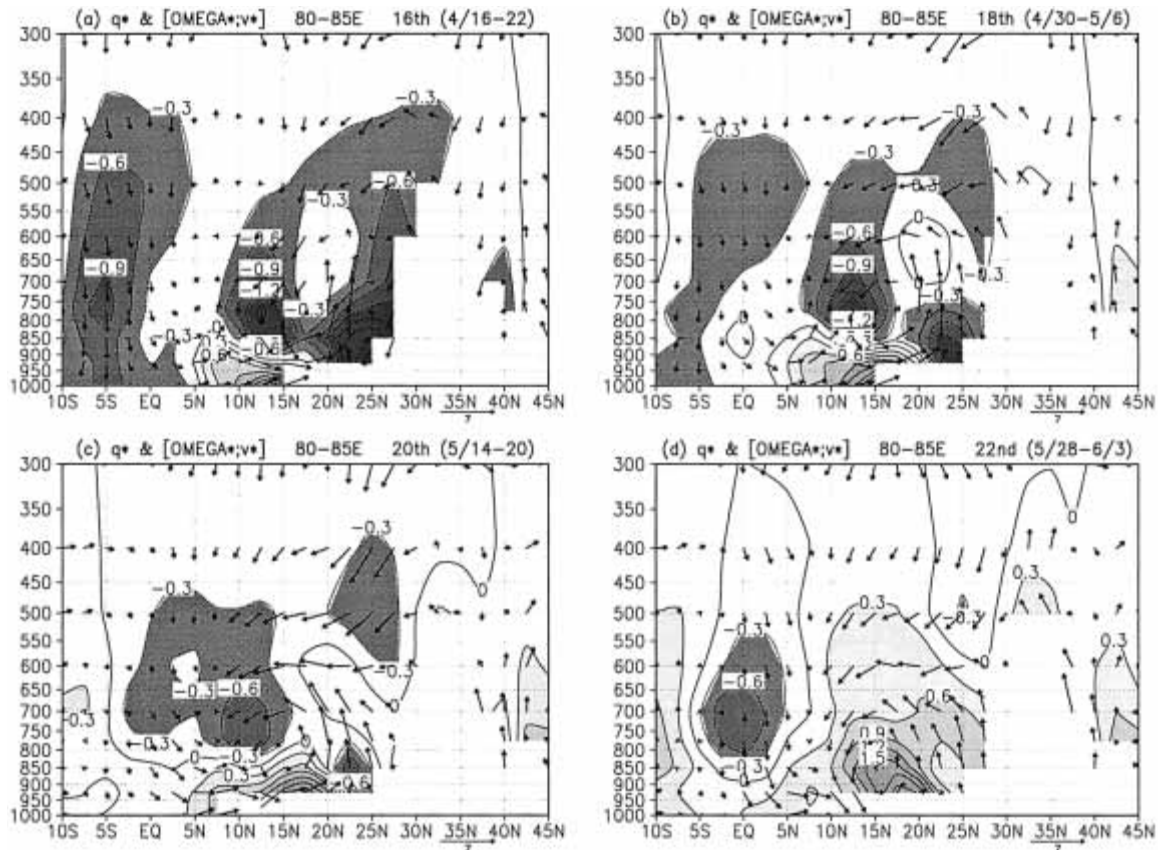


Fig. 7. As in Fig. 6 but for vertical  $p$ -velocity  $\omega^*$ , meridional wind  $v^*$  and mixing ratio  $q^*$ . Contour interval is  $0.3 \text{ g kg}^{-1}$ . Heavy and light shadings denote significant negative and positive mixing ratio anomalies, respectively.

any significant vertical circulations, in the vicinity of the Tibetan Plateau between  $80^\circ$  and  $85^\circ\text{E}$  are not seen.

Figure 7 is the same as Fig. 6 but for zonally asymmetric anomalies. The shallow vertical circulation is evident in the lower troposphere between  $10^\circ$  and  $25^\circ\text{N}$ . Negative  $q^*$  appears at the 700-hPa level or so, between  $10^\circ$  and  $15^\circ\text{E}$  from middle April to middle May, along with descent anomalies. This corresponds to the negative  $q^*$  over the Bay of Bengal as shown in Fig. 5. Thus, the establishment of the shallow vertical circulation leads to the dry intrusion into the layer at 600–850 hPa over the Bay of Bengal through advective processes, especially vertical advection. On the other hand, positive  $q^*$  with anomalous southerlies amplifies in the boundary layer at almost the same latitudes, contributing to the reinforcement of the vertical

gradient of mixing ratio in the lower troposphere. After the onset (Fig. 7d), positive  $q^*$  areas rapidly extend upward to the upper troposphere, and negative  $q^*$  areas seen at around 700-hPa become dissipated. Looking at Fig. 6 again, in fact, the vertical gradient of the mixing ratio in the lower troposphere considerably weakens at the post-onset regime, compared to that at the pre-onset regime.

The height-latitude sections of anomalous temperature  $T^*$  averaged between  $80^\circ$  and  $85^\circ\text{E}$ , are also shown in Fig. 8, along with both  $\omega$  and  $v$ . Note that vertical  $p$ -velocity and meridional wind are not zonally asymmetric anomalies to look at the behavior of Hadley circulation in the upper troposphere in the simplest manner. The center of very warm  $T^*$  is located at near surface of the inland between  $20^\circ$  and  $25^\circ\text{N}$  prior to the onset and its maxi-

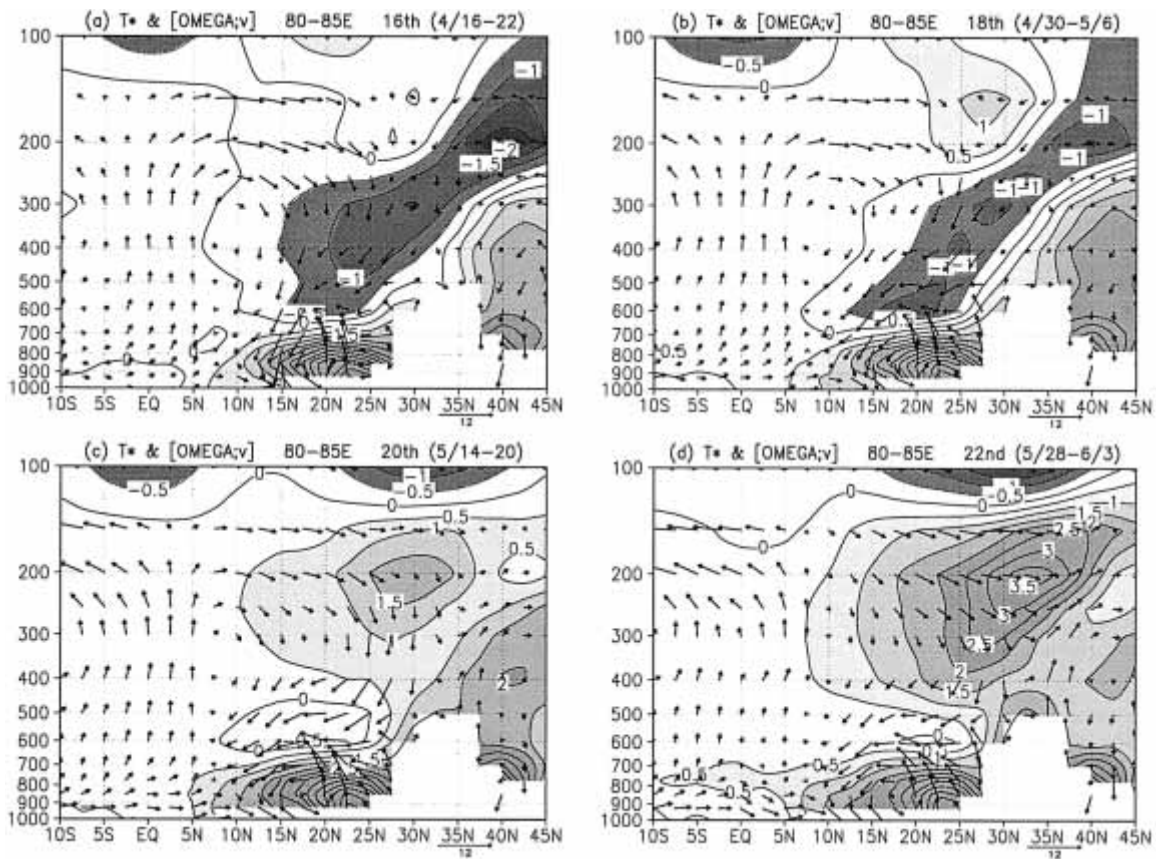


Fig. 8. Height-latitude sections of anomalous temperature  $T^*$  below 100-hPa averaged from  $80^\circ$  to  $85^\circ\text{E}$  for: (a) 16<sup>th</sup> week (April 16–22); (b) 18<sup>th</sup> week (April 30–May 6); (c) 20<sup>th</sup> week (May 14–20); and (d) 22<sup>nd</sup> week (May 28–June 3). Contour interval is  $0.5^\circ\text{C}$ . Also shown are climatological mean vertical  $p$ -velocity  $\omega$  and meridional wind  $v$ . The vertical motion has been exaggerated 75 times.

imum value is about  $+6.0^\circ\text{C}$ . The warm anomalies involve dry thermal convection, and reach up to the 700-hPa level. The dry thermal convection is capped with the subsiding branch of the Hadley circulation. These features are strongly suggestive of an indispensable role of thermal forcing by land surface warming in originating the shallow vertical circulation over the subcontinent.

Over the region north of the Tibetan Plateau, another warm  $T^*$  expands into the upper troposphere, which may also be attributed to the land surface warming on a continental scale. Although cool anomalies appear in the upper troposphere over the subcontinent from middle April to early May, alternated warm anomalies begin to dominate after that. The center of this warming, accompanied by southerly wind and

descending motion, is located at the 200-hPa level and its vicinity. One may wonder why such warming is observed just below the tropopause. This might be associated with the monsoon onset, which will be discussed later.

We made height-latitude sections along the western coast of the Indian subcontinent as well as its eastern coast, but could not find any significant shallow vertical circulations. As previously stated, an abrupt onset is also observed in Region C as well as Region B. In the next subsection, height-longitude sections across Region C are presented.

#### 4.3 Height-longitude sections

Figure 9 shows the height-longitude sections of anomalous mixing ratio  $q^*$  averaged from  $10^\circ$  to  $15^\circ\text{N}$  across southern India and Indochina,

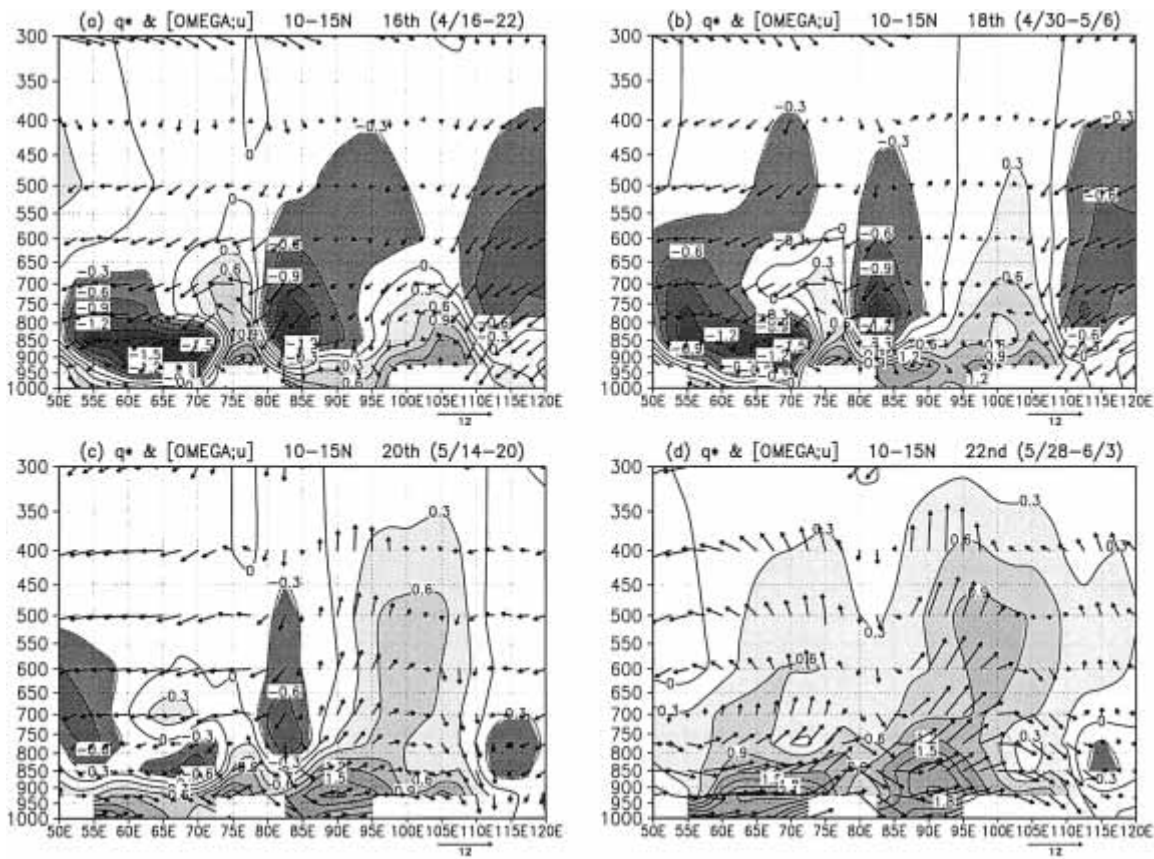


Fig. 9. Height-longitude sections of anomalous mixing ratio  $q^*$  below 300-hPa averaged from  $10^\circ$  to  $15^\circ\text{N}$  for: (a) 16<sup>th</sup> week (April 16–22); (b) 18<sup>th</sup> week (April 30–May 6); (c) 20<sup>th</sup> week (May 14–20); and (d) 22<sup>nd</sup> week (May 28–June 3). Contour interval is  $0.3 \text{ g kg}^{-1}$ . Also shown are climatological mean vertical  $p$ -velocity  $\omega$  and zonal wind  $u$ . The vertical motion has been exaggerated 75 times.

along with vertical  $p$ -velocity  $\omega$  and zonal wind  $u$ . In middle April remarkable positive  $q^*$  areas extend up to the 700-hPa level or so, over both the subcontinent and the Indochina peninsula, accompanied by ascending motion. Deep moist convection is established over the peninsula by middle May, which corresponds to the earliest onset of the South Asian summer monsoon. Negative  $q^*$  seen around 700–850 hPa in the eastern coast of the subcontinent corresponds to the descending branch of the north-south shallow vertical circulation (Fig. 7). Looking at the Arabian Sea, negative  $q^*$  dominates at 850-hPa and its vicinity prior to the second onset. An east-west shallow vertical circulation can be seen between the subcontinent and the Arabian Sea. However, its subsiding branch in the western coast of the subcontinent is disrupted

by early June. In early June, distinctive positive  $q^*$  expands upward over both the Bay of Bengal and the Arabian Sea along with ascending motion, implying the prominence of deep moist convection.

Thus, this figure clearly shows the behavior of east-to-west successive onsets of the Asian summer monsoon system. Pronounced negative  $q^*$  is present above the boundary layer over the Bay of Bengal and the Arabian Sea from early May to middle May prior to the second onset, and pre-onset conditions in Region C is similar to those in Region B in terms of the presence of shallow vertical circulation.

### 5. SST and convective instability

Figure 10 shows the spatial patterns of  $SST^*$  for: (a) 16<sup>th</sup> week; (b) 18<sup>th</sup> week; (c) 20<sup>th</sup>

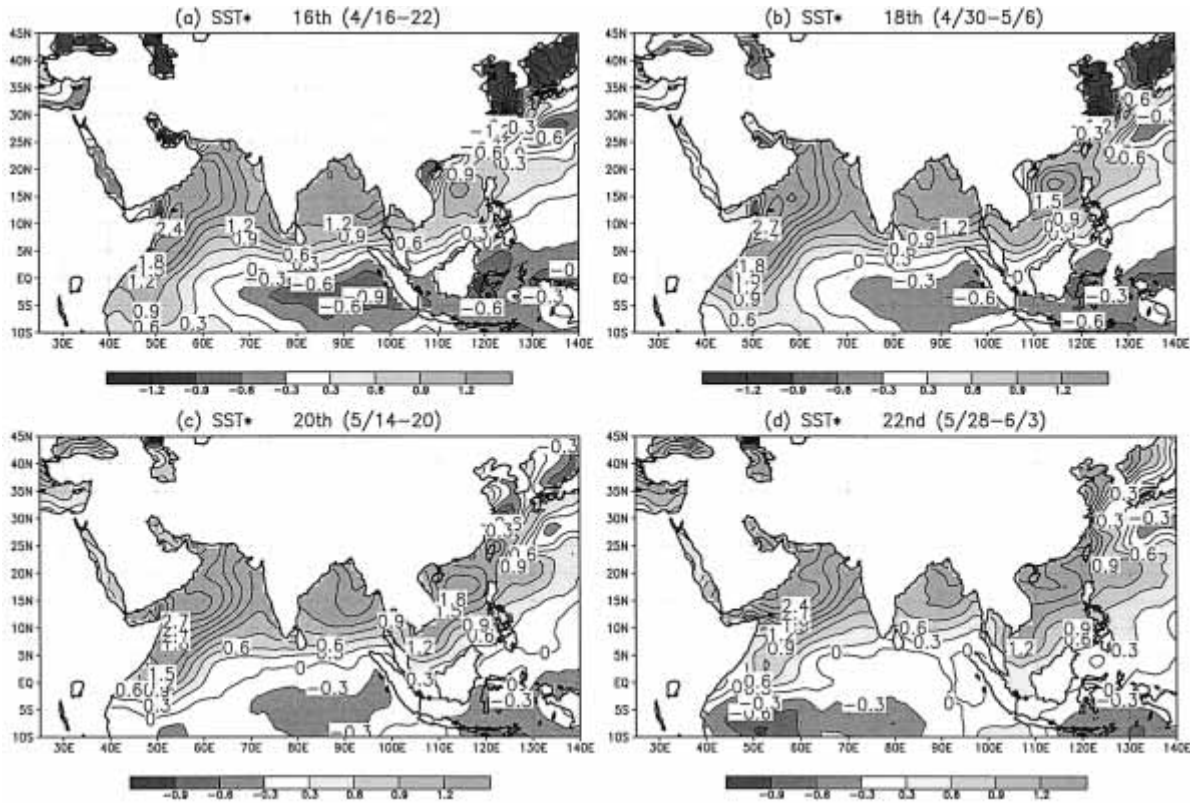


Fig. 10. Spatial patterns of  $SST^*$  for: (a) 16<sup>th</sup> week (April 16–22); (b) 18<sup>th</sup> week (April 30–May 6); (c) 20<sup>th</sup> week (May 14–20); and (d) 22<sup>nd</sup> week (May 28–June 3). Contour interval is 0.3°C.

week; and (d) 22<sup>nd</sup> week. In all panels, positive anomalies are evident over the Arabian Sea, the Bay of Bengal, and the South China Sea. In particular,  $SST^*$  reaches a value of greater than 2.0°C in the western section of the Arabian Sea. Kawamura et al. (2002) showed that the presence of the Australian continent itself produces a warming in SST over the ocean off the equatorial side of the continent, prior to the onset of summer monsoon, through land-atmosphere-ocean interactive processes. The SST warming is primarily due to decreased surface evaporation and increased solar radiation by less cloud cover, associated with establishment of continental-scale shallow vertical circulation. It is anticipated that similar processes dominate over the Arabian Sea, the Bay of Bengal and the South China Sea prior to the onset of the South Asian summer monsoon. In fact, positive  $SST^*$  areas coincide well with attenuated surface wind areas (figure not shown).

Suppressed vertical mixing in the surface layer of the ocean by decreased wind speed may also contribute to the SST increase, especially in the western portion of the Arabian Sea.

It is also seen that the magnitude of positive  $SST^*$  values over the Bay of Bengal become somewhat small once the summer monsoon commences. This may be attributed to the abrupt change in net surface heat flux before and after the monsoon onset. For instance, Shaji et al. (2003) pointed out that the time tendency of near-surface heat budget in the Bay of Bengal depends mainly on the net surface heat flux.

The appreciable SST warming over those regions acts toward the increase in equivalent potential temperature,  $\theta_e$ , at the lowest level. On the other hand, the establishment of the shallow vertical circulation leads to the dry intrusion into the layer at about 700-hPa, especially over the Bay of Bengal through advective

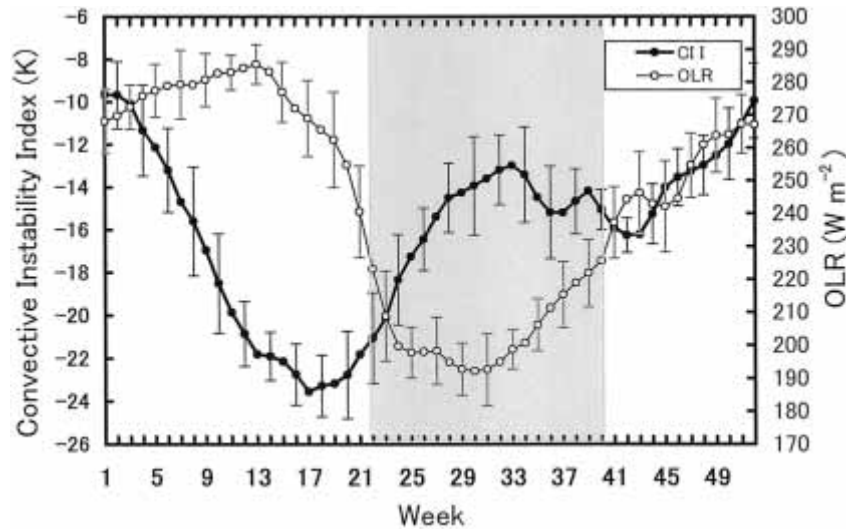


Fig. 11. Seasonal evolution of a potentially convective instability index, defined as the difference of equivalent potential temperature between 700- and 1000-hPa, for Region B (thick line). Also indicated is that of OLR (thin line) along with its standard deviation. Shaded area denotes summer monsoon season.

processes, as shown in Fig. 7. A combination of these processes is very likely to create a more potentially unstable condition in the lower troposphere prior to the monsoon onset. The vertical gradient of  $\theta_e$  provides an appropriate measure of potentially convective instability in the lower troposphere. Thus, a potentially convective instability index is defined as the difference of  $\theta_e$  between 700- and 1000-hPa. As a typical case, we present Fig. 11, showing the seasonal evolution of the convective instability index for Region B, along with OLR. Considering the seasonal evolution of OLR, the summer monsoon in that region commences around the 22<sup>nd</sup> week and retreats around the 40<sup>th</sup> week. The instability index becomes low rapidly from boreal winter to spring and reaches its minimum at the 17<sup>th</sup> week. Extremely low values persist until the 20<sup>th</sup> week. Once the onset occurs, the index begins to increase and its increase continues until the 33<sup>rd</sup> week. It also turns out that there is a remarkable difference of the instability index between the onset and retreat phases. This strongly suggests that appearance of the strong convective instability during the premonsoon period is prerequisite for the occurrence of the abrupt onset, eventually bringing about the asymmetry of the tran-

sition speed between the onset and retreat phases. Figure 12 shows the differences of  $\theta_e$  between 700-hPa and 1000-hPa for: (a) 16<sup>th</sup> week, (b) 18<sup>th</sup> week, (c) 20<sup>th</sup> week, and (d) 22<sup>nd</sup> week. We find, indeed, that potentially convective instability becomes strong over the Bay of Bengal from middle April to middle May. The potentially convective instability is more evident over the western part of the Bay of Bengal, especially along the eastern coast of the subcontinent. After the Indian summer monsoon commences, the vertical gradient of  $\theta_e$  is somewhat small compared to that before the onset. The lower troposphere over the Arabian Sea also has a potentially unstable condition, although there is a significant phase difference in the peak period of convective instability between the Arabian Sea and the Bay of Bengal.

Figure 13 shows the spatial distributions of moisture flux divergence at 925-hPa level. An important feature is that, prior to the onset, the flux divergence prevails over the surrounding oceans of the subcontinent, whereas the convergence appears over the inland. Since subsidence dominates at 850-hPa level in the periphery of the subcontinent (figure not shown), the flux divergence at 925-hPa is induced by the descending motion that is part of a sub-

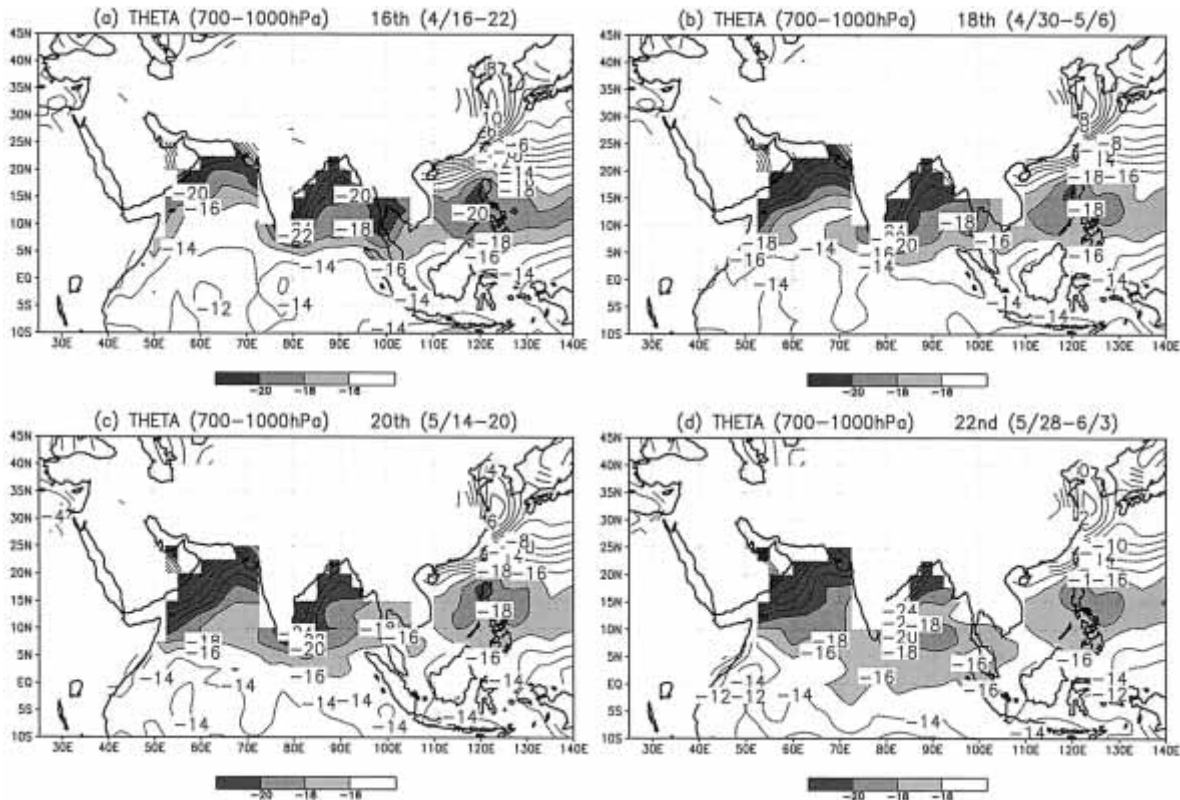


Fig. 12. Differences of equivalent potential temperature between 700- and 1000-hPa for: (a) 16<sup>th</sup> week (April 16–22); (b) 18<sup>th</sup> week (April 30–May 6); (c) 20<sup>th</sup> week (May 14–20); and (d) 22<sup>nd</sup> week (May 28–June 3). Contour interval is 2 K. Shading denotes regions of less than  $-16$  K, indicating enhanced convective instability.

continental scale shallow vertical circulation. While the subsidence inhibits convection and increases incoming solar radiation into the ocean, potentially convective instability is further enhanced (Fig. 12). Such pre-onset conditions are very similar to those seen in the Australian summer monsoon system (Kawamura et al. 2002). Of course, this instability is potential and an external source of energy has to be supplied to the air mass to convert its instability into actual instability (Emanuel 1994). If large-scale disturbances with ascending motion arrive at the region where the lower troposphere is potentially unstable, deep cumulus convection is able to break out suddenly. Once the summer monsoon commences, pronounced low-level moisture flux convergence can also be seen over the Bay of Bengal and the Arabian Sea (Fig. 13d).

## 6. Discussion

### 6.1 Why is the onset over the Indochina peninsula relatively slow?

It is interesting to note that a shallow vertical circulation is not organized very well over the Indochina peninsula during the premonsoon period (figure not shown). Kawamura et al.'s onset mechanism does not operate without establishment of the shallow vertical circulation. Thus, the monsoon onset over that region is more likely to depend strongly on the seasonal migration of ITCZ over tropical oceans. As inferred from Fig. 2a, its seasonal migration is comparatively slow. Kanai et al. (2002) postulated that the earliest onset over Indochina and its vicinity could be interpreted as the onset of marine monsoon. They also pointed out that the onset requires the warm SST

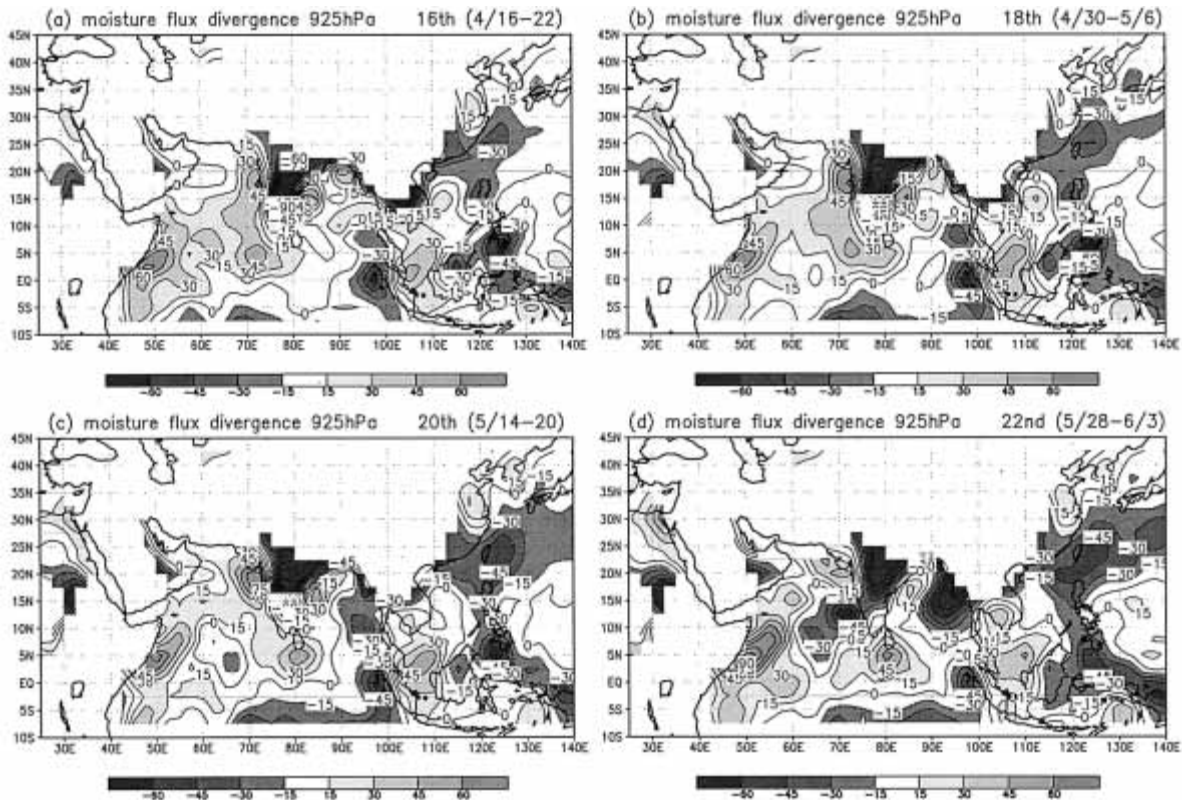


Fig. 13. Spatial patterns of moisture flux divergence at 925-hPa for: (a) 16<sup>th</sup> week (April 16–22); (b) 18<sup>th</sup> week (April 30–May 6); (c) 20<sup>th</sup> week (May 14–20); and (d) 22<sup>nd</sup> week (May 28–June 3). Contour interval is  $15 \times 10^{-6} \text{ g kg}^{-1} \text{ s}^{-1}$ .

in the vicinity of the Indochina peninsula. Although their interesting work emphasizes marine monsoon-like features, it should also be noted here that the presence of the Asian continent itself contributes to the rapid increase in SST around Indochina prior to the onset through land-atmosphere-ocean interactive processes.

It is unclear why a shallow vertical circulation does not necessarily dominate over the Indochina peninsula. Looking at Fig. 4 again, moisture transport from the tropics into Southeast Asia is already intensified in middle April. This is intimately associated with enhancement of low-level southerly flow along the eastern coast of the continent due to land-ocean thermal contrast. Once a continental-scale thermal low is established, it is expected that much moisture from the tropics is supplied in the southeastern portion of the continent. Since the Indochina peninsula is much smaller

than the entire Asian continent, large-scale premonsoon flow over Indochina might be more sensitive to the continental-scale topography than local topography. If this is true, much moisture can easily intrude into the inland of Indochina along the western periphery of a high over the western Pacific, facilitating the earliest monsoon onset. This issue requires further clarification.

### 6.2 Does the Tibetan Plateau contribute to the abrupt onset?

The Asian continent is very different from the Australian continent in terms of the presence of high mountains like the Tibetan Plateau. Some researchers emphasize that rapid land-surface warming in the Tibetan Plateau may contribute to the abrupt onset of the South Asian summer monsoon (e.g., Ueda and Yasunari 1998). Figure 14 shows the spatial patterns of anomalous temperature  $T^*$  and wind

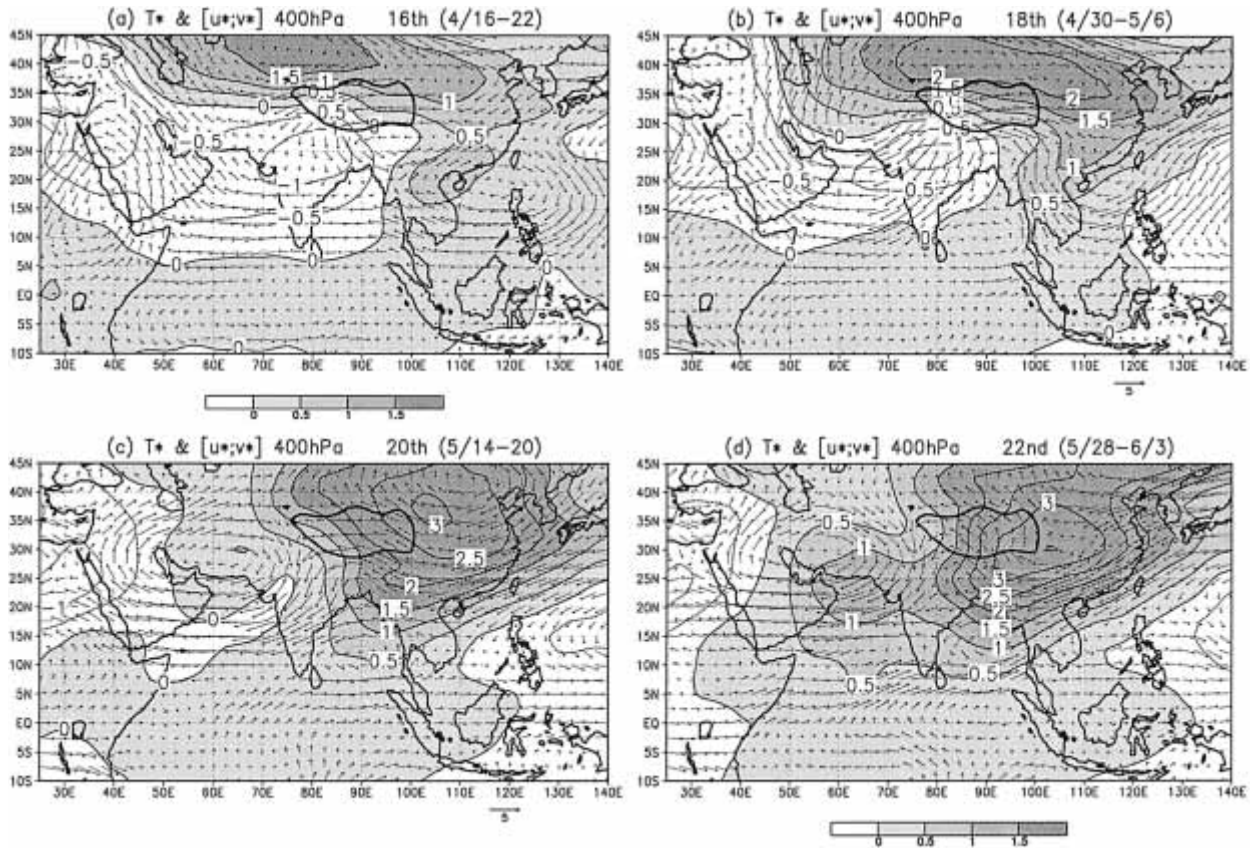


Fig. 14. Spatial patterns of anomalous 400-hPa temperature  $T^*$  and wind vector ( $u^*, v^*$ ) for: (a) 16<sup>th</sup> week (April 16–22); (b) 18<sup>th</sup> week (April 30–May 6); (c) 20<sup>th</sup> week (May 14–20); and (d) 22<sup>nd</sup> week (May 28–June 3). Contour interval for temperature is 0.5°C, and reference arrow is 5 m s<sup>-1</sup>. Shading denotes regions of positive temperature anomalies.

vector ( $u^*, v^*$ ) at 400-hPa level above the Tibetan Plateau for (a) 16<sup>th</sup> week, (b) 18<sup>th</sup> week, (c) 20<sup>th</sup> week, and (d) 22<sup>nd</sup> week. From middle May to the beginning of June, the center of positive  $T^*$  area exceeding a value of +3°C is located to the east of the Tibetan Plateau, and positive anomalies cover the eastern portion of the Asian continent. Ueda et al. (2002) pointed out that the eastern Tibetan Plateau remains a heat sink in the first transition of the South Asian summer monsoon, using the GAME 4DDA upper-air data. If this is a common feature although their analysis is based only to the 1998 case, we may think it very difficult that the distinctive warming at 400-hPa east of the Tibetan Plateau seen in middle May depends strongly on sensible heat supply from the land surface of the eastern Plateau. Even though the

rapid land-surface warming occurs in the Tibetan Plateau during the first transition, its influence is not necessarily predominant in the 400-hPa temperature distribution, compared to thermal forcing by land-surface warming in the other regions of the continent.

On the other hand, remarkable positive anomalies appear suddenly at 200-hPa level just over the Tibetan Plateau in middle May when the earliest onset occurs over Indochina (see Fig. 8c). However, the center of this warming is accompanied by southerly flow and subsiding motion, and is clearly isolated from another warming north of the Tibetan Plateau. Thus, the warming at 200-hPa can hardly be interpreted as a result of enhanced sensible heat flux due to the land-surface warming of the Tibetan Plateau. It is anticipated that the



sudden warming at 200-hPa over the Plateau is the result rather than the cause of the earliest onset of the Indochina monsoon. Presumably, vertical and horizontal advective processes of temperature relevant to deep moist convection play a significant role in warming the layer around the tropopause over the Plateau. It is agreed, of course, that the Tibetan Plateau plays an important role in strengthening the South Asian summer monsoon activity (e.g., Hahn and Manabe 1975; Yanai et al. 1992). However, if the above features are considered, it does not seem that the presence of the Tibetan Plateau is prerequisite for the abruptness of monsoon onset in terms of its surface heat effect.

## 7. Summary

To validate whether the onset mechanism proposed by Kawamura et al. (2002) can apply to other monsoon systems, we investigated the two successive onsets of the South Asian summer monsoon system, using the European Centre for Medium-Range Weather Forecasts reanalysis data. Four major regions were selected: i.e., Southeast Asia, the western portion of the Bay of Bengal, including part of the eastern coast of the Indian subcontinent, the eastern Arabian Sea including part of the western coast of the subcontinent, and an inland area of the subcontinent. Abruptness of the onset is most evident over the coastal regions of the subcontinent. The asymmetry of the transition speed between the onset and retreat regimes is also apparent in the coastal regions, but is less clear in the other regions. It is found that premonsoon circulations over the Indian subcontinent, and adjacent oceans, are very similar to those observed prior to the onset of the Australian summer monsoon. It is also confirmed that a combination of the SST increase and dry intrusion into the layer at 600–850 hPa level over the surrounding oceans, plays a vital role in enhancing potentially convective instability prior to the onset of the Indian summer monsoon. Thus, their onset mechanism can apply to the abrupt onset of the Indian summer monsoon. On the other hand, a shallow vertical circulation is not organized very well over the Indochina peninsula during the premonsoon period. Since the onset mechanism does not operate without establishment of

the shallow vertical circulation, it cannot apply to the onset of the Indochina summer monsoon, which is consistent with the observational fact that Indochina is characterized by a relatively slow onset, although its date is earliest. Conversely, the onset of the Indian summer monsoon is delayed because subsidence in the periphery of a sub-continental scale thermal low, resulting from intensification of land-ocean thermal contrast, inhibits convection. These differences may be one of the possible reasons why the two major onsets seen in the South Asian summer monsoon system are clearly distinguished from each other.

This study also shows the regional differences of the time evolution of the South Asian summer monsoon due to complicated topography of the continent. Further physical understanding of the complicated monsoon system is expected by applying the analysis procedure used in this study to thermodynamic parameters, such as the apparent heat source and apparent moisture sink. Another important issue is how the presence of a continent affects the subsurface temperature and circulation fields in the surrounding oceans through dynamic and thermodynamic processes during the premonsoon period. An atmosphere-ocean coupled model will also be a useful tool for addressing such an issue.

## Acknowledgments

The authors are grateful to Takio Murakami, Shang-Ping Xie, Jun Matsumoto and Masato Shinoda for stimulating discussions. Comments by Tomoaki Ose and two anonymous reviewers were extremely helpful. This research was supported by the research project “Refinement of numerical modeling and technology of global and regional water cycle”, and Grants-in-Aids (14540406) of the Japanese Ministry of Education, Sports, Culture, Science and Technology; and by the Mitsubishi Foundation for the Promotion of Science.

## References

- Chao, W.C., 2000: Multiple quasi equilibria of the ITCZ and the origin of monsoon onset. *J. Atmos. Sci.*, **57**, 641–651.
- Emanuel, K.A., 1994: *Atmospheric convection*. Oxford University Press, 580pp.

- Hahn, D.G. and S. Manabe, 1975: The role of mountains in the south Asian monsoon circulation. *J. Atmos. Sci.*, **32**, 1515–1541.
- He, H., J.W. McGinnis, Z. Song and M. Yanai, 1987: Onset of the Asian monsoon in 1979 and the Effect of the Tibetan Plateau. *Mon. Wea. Rev.*, **115**, 1966–1995.
- Holland, G.J., 1986: Interannual variability of the Australian summer monsoon at Darwin: 1952–82. *Mon. Wea. Rev.*, **114**, 594–604.
- Hsu, H.-H., C.-T. Terng and C.-T. Chen, 1999: Evolution of large-scale circulation and heating during the first transition of Asian summer monsoon. *J. Climate*, **12**, 793–810.
- Kanae, S., T. Oki and K. Musiaka, 2002: Principal condition for the earliest Asian summer monsoon onset. *Geophys. Res. Lett.*, **29**, 10.1029/2002GL015346.
- Kawamura, R. and T. Murakami, 1998: Baiu near Japan and its relation to summer monsoons over Southeast Asia and the western North Pacific. *J. Meteor. Soc. Japan*, **76**, 619–639.
- , Y. Fukuta, H. Ueda, T. Matsuura and S. Iizuka, 2002: A mechanism of the onset of the Australian summer monsoon. *J. Geophys. Res.*, **107**, 10.1029/2001JD001070.
- Krishnakumar, V. and K.-M. Lau, 1998: Possible role of symmetric instability in the onset and abrupt transition of the Asian monsoon. *J. Meteor. Soc. Japan*, **76**, 363–383.
- Krishnamurti, T.N. and Y. Ramanathan, 1982: Sensitivity of the monsoon onset to differential heating. *J. Atmos. Sci.*, **39**, 1290–1306.
- Lau, K.-M. and M.T. Li, 1984: The monsoon of East Asia and its global association—a survey. *Bull. Amer. Meteor. Soc.*, **65**, 114–125.
- , G. Yang and S.H. Shen, 1988: Seasonal and intraseasonal climatology of summer monsoon rainfall over East Asia. *Mon. Wea. Rev.*, **116**, 18–37.
- Li, C. and M. Yanai, 1996: The onset and interannual variability of the Asian summer monsoon in relation to land-sea thermal contrast. *J. Climate*, **9**, 358–375.
- Lubis, S.M. and T. Murakami, 1984: Moisture budget during the 1978–79 Southern Hemisphere summer Monsoon. *J. Meteor. Soc. Japan*, **62**, 748–760.
- Matsumoto, J., 1997: Seasonal transition of summer rainy season over Indochina and adjacent monsoon region. *Adv. Atmos. Sci.*, **14**, 231–245.
- Murakami, T. and T. Nakazawa, 1985: Transition from the Southern to Northern Hemisphere summer monsoon. *Mon. Wea. Rev.*, **113**, 1470–1486.
- Nicholls, N., J.L. McBride and R.J. Ormerod, 1982: On predicting the onset of the Australian wet season at Darwin. *Mon. Wea. Rev.*, **110**, 14–17.
- Reynolds, R.W. and T.M. Smith, 1994: Improved global sea surface temperature analyses using optimum interpolation. *J. Climate*, **7**, 929–948.
- Shaji, C., S. Iizuka and T. Matsuura, 2003: Seasonal variability of near-surface heat budget of selected oceanic areas in the north tropical Indian Ocean. *J. Oceanogr.*, **59**, 87–103.
- Suppiah, R., 1992: The Australian summer monsoon: a review. *Progress in Physical Geography*, **16**, 283–318.
- Ueda, H. and T. Yasunari, 1998: Role of warming over the Tibetan Plateau in early onset of the summer monsoon over the Bay of Bengal and the South China Sea. *J. Meteor. Soc. Japan*, **76**, 1–12.
- , H. Kanamori and N. Yamazaki, 2002: Seasonal contrasting features of heat and moisture budgets between the eastern and western Tibetan Plateau during the GAME IOP. (Submitted to *J. Climate*).
- Xie, S.P. and N. Saiki, 1999: Abrupt onset and slow seasonal evolution of summer monsoon in an idealized GCM simulation. *J. Meteor. Soc. Japan*, **77**, 949–968.
- Yanai, M., C. Li and Z. Song, 1992: Seasonal heating of the Tibetan Plateau and its effects on the evolution of the Asian summer monsoon. *J. Meteor. Soc. Japan*, **70**, 319–351.
- Yano, J.-I. and J.L. McBride, 1998: An aquaplanet monsoon. *J. Atmos. Sci.*, **55**, 1373–1399.